Periodica Polytechnica
Civil Engineering

62(4), pp. 992–1000, 2018
https://doi.org/10.3311/PPci.12247

Effect of Roof and Diaphragm Connectivity on Dynamic Behaviour of the PP-band Retrofitted Adobe Masonry Structures

Navaratnarajah Sathiparan[1,2*]

RESEARCH ARTICLE

Received 20 March 2018; Revised 23 May 2018; Accepted 09 July 2018

Abstract

This paper discusses the shaking table test results of three PP-band (Polypropylene band) retrofitted quarter scale one-story masonry house models with different roof conditions. Better connections between masonry wall and roof connection are one factor to improve the seismic safety of the masonry houses. Past studies show that PP-band retrofitting improves the integrity of structural components and prevent the collapse of masonry structures during an earthquake. Although the effect of masonry unit type, surface plastering, the pitch of the PP-band mesh, PP-band connectivity in mesh and tightness of the mesh attachment to walls were studied by experiment program, the effect of the roof and its diaphragm connectivity on PP-band retrofitted masonry structure is non-existent. Therefore, an experimental program was designed and executed for an understanding the effect of the roof and its connection on the dynamic behavior of the PP-band retrofitted box-shaped masonry house models. Results reveal that the PP-band retrofitted models with proper roof diaphragm improves the seismic behavior with respect to lateral drift, shear resistance and ductility.

Keywords

PP-band retrofitting, adobe masonry, roof diaphragm, earthquakes

1 Senior Lecturer, Department of Civil Engineering,
Faculty of Engineering,
University of Jaffna
Kilinochchi, Sri Lanka
2 Former JSPS Post-Doctoral Fellow,
Institute of Industrial Science,
The University of Tokyo, Japan
* Corresponding author, email: sakthi@eng.jfn.ac.lk

1 Introduction

Most of the human fatalities during earthquakes in developing countries occur due to the collapse of low earthquake-resistant masonry houses [1]. Therefore, retrofitting of these types of masonry structures is the key issue for earthquake disaster mitigation in developing countries to reduce the casualties significantly. A number of retrofitting techniques have been developed for low earthquake-resistant, non-engineering masonry structures. However, people living in these types of houses have limited resources in the sense of financial support, construction technology and manpower. Therefore, when proposes a retrofitting technique, it should be low cost with the locally available material, applicable with low technical knowledge and culturally acceptable. Retrofitting masonry structures using PP-band (polypropylene band) meshes satisfies these requirements. PP meshing uses common PP packaging straps (PP bands) to form a mesh, which is then used to encase masonry walls by fixing to both faces of walls. The mesh prevents the separation of structural elements and the escape of debris, maintaining sufficient structural integrity to prevent collapse [2]. Past studies show that PP-band retrofitting improves the integrity of structural components and prevent the collapse of masonry structures during an earthquake [3–7].

Experimental programs on PP-band retrofitting technique for in-plane and out-of-plane test on masonry wallets [3,8], shaking table test on a reduced scale masonry house models [4–6] and shaking table test of full-scale house models [7] have shown that PP-band retrofitting improves the seismic performance of the unreinforced masonry structures. These studies have also shown that, during moderate earthquakes, PP-band meshes can provide enough seismic resistance to guaranty limited and controlled cracking. Also, during strong earthquakes, they are expected to prevent or delay the collapse of the masonry structures. PP-band mesh retrofitting has had applications in China, Nepal, Pakistan, and Indonesia [9]. Past studies show that the performance of the PP-retrofitting structure is influenced by the pitch width of the mesh, tightness of the mesh attachment, materials used for surface plastering [10], the strength of the masonry unit [11] and PP-band mesh

connectivity [12]. However, the effect of the roof and its diaphragm connectivity on PP-band retrofitted masonry structure is non-existent. Hence, the current research was designed and undertaken to determine the dynamic behavior of the PP-band retrofitted masonry under various roof conditions.

Better connection between masonry wall and roof connection is one of the factors to improve the seismic safety of the masonry houses. Holding the disintegrated elements together to preventing the collapse is depending on the connection between the roof or floor and walls, between intersecting walls, and the wall and foundation. For a house without a roof, when the connection between adjacent wall is weak, the walls fail in out-of-plane mode failure mechanisms. Generally, this type of failure is brittle. In the case of proper roof connections, lateral loads are distributed to the walls in proportion to their stiffness. Therefore, possible failure types are sliding shear, diagonal shear or rocking. In this case, it allows more energy dissipation before the collapse than the house without a roof.

Past studies show that structure with a proper roof connection provides the better seismic performance with respect to lateral drift, shear resistance and ductility [13–15]. Magenes et al. [16] reported the out-of-plane behavior of unreinforced masonry walls subjected to dynamic loading. Unreinforced masonry walls were subjected to dynamic actions orthogonal to their plane, resulting from simulated earthquake motions on a shake table was reported in this study. Results show that diaphragm flexibility significantly increased the out-of-plane displacement response and adequate anchorage of unreinforced masonry walls to the diaphragm is critical to preventing out-of-plane failure.

Langroudi et al. [17] conducted a case study to evaluate the effects of roof diaphragm on the seismic behavior of unreinforced masonry buildings. Finite element modeling of a two-story masonry building was chosen for this study. Results show that diaphragm flexibility has a significant effect on the base shear force distribution to the unreinforced masonry structures. Also, the results show that the seismic response of the masonry structures with the rigid diaphragm is better than with a flexible diaphragm with respect to yield displacement, lateral stiffness, shear resistance and ductility.

Sathiparan [18] has tested quarter scale unreinforced masonry structures with different roof conditions subjected to dynamic loading. Results show that the box behavior of the roof and connectivity of roofs to wall influences the type of failure modes. House with a proper roof connection demonstrates a more global response, but house model without a roof and house model with lesser connectivity show out-of-plane failure mechanisms. Also, results reveal that the model with a proper roof diaphragm improves the seismic behavior with respect maximum lateral drift, shear resistance, stiffness, and ductility. In this study, the global failure of unreinforced masonry is initiated by the local failure of the wall itself (Out of plane failure of the wall in the perpendicular direction to shaking and sliding or diagonal shear failure in the wall in the direction of shaking). However, when masonry structure is retrofitted by PP-band mesh, the local failure is prevented. Therefore, it is except that roof diaphragm and its connectivity effect on retrofitted masonry house is different from unreinforced masonry. Based on that, in present study focus roof diaphragm and its connectivity effect on PP-band retrofitted masonry house models.

The main reason that motivated the present study was the scarce experimental information on the roof and its connection to a wall effect on mesh type retrofitted masonry structure. Therefore, an experimental program was designed for an understanding of the roof and its connection effect on the dynamic behavior of the PP-band retrofitted masonry house models by a sequence of shaking table tests. One-quarter scale one-story adobe masonry house model and three different roof conditions were adopted for this study.

2 Experimental program

2.1 Specimen description and construction

A quarter-scale one-story box shape house is used as the subject of this investigation. The house was 993 mm × 993 mm in plans with a wall height and a thickness of 720 mm and 50 mm, respectively. The dimension of the house models is presented in Fig 1.

The objectives of the tests on house models were to determine the effects of the roof and it diaphragm connectivity on the dynamic behavior of the PP-band retrofitted masonry structures. Considering that three models of simple buildings were constructed in this experimental program with following specifications;

- Model 1: A box-type one-story building without a roof.
- Model 2: A box-type one-story building with a timber roof and the roof is connected to north and south walls.
- Model 3: A box-type one-story building with a timber roof and the roof is connected to all four walls.

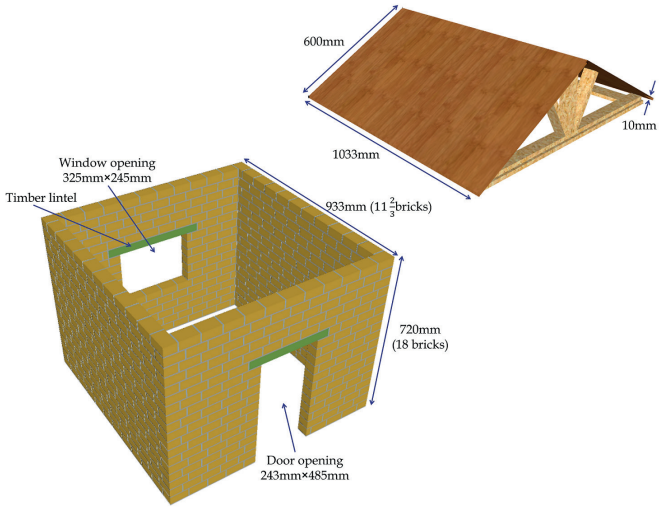

Fig. 1 Dimension of the house model

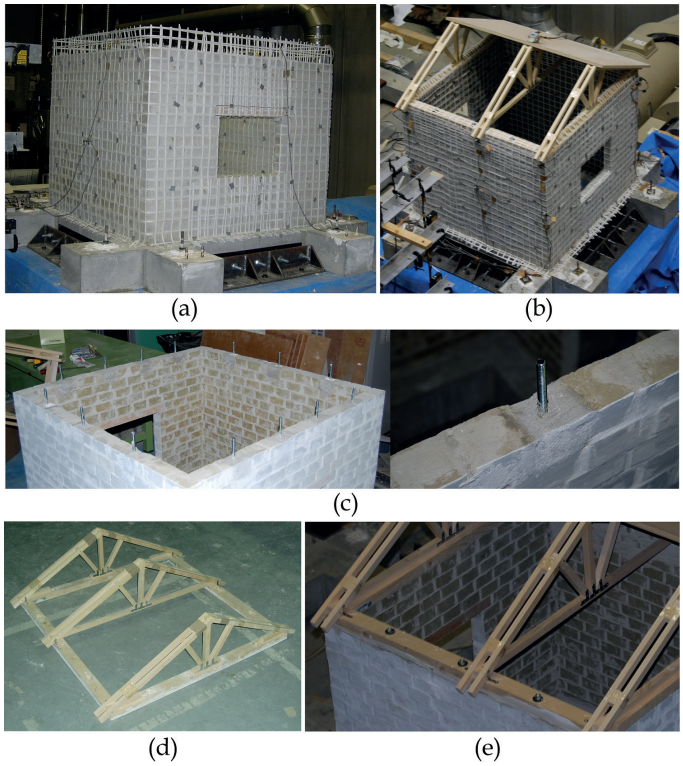

Fig. 2 Structural components of the house model (a) top layer of the house model for roof connection (b) roof frame, and (c) house model and roof connections

A reinforced concrete pad was designed and constructed to provide a foundation and strong mortar was used between the foundation and first adobe unit layer of the specimen for a proper connection between house model and foundation. For strong mortar, the cement-sand ratio of 1:3 mortar with a cement/water ratio of 0.6 was provided. Each side wall consisted of 11 adobe units per layer and 18 rows along the height. For roof structure, timber truss frame attached to two inclined plywood sheets with a dimension of 1033 mm × 600 mm and 10 mm thick was adopted. Plywood sheets nailed to the sloping edges of the truss. The roof frame was connected to the walls using 10 mm diameter bolt and nut at 160 mm intervals as shown in Fig. 2(a), 2(b) and 2(c). In between masonry walls and roof frame, 5 mm thick cement-sand ratio of 1:8 mortar with a cement/water ratio of 0.7 was provided. Mortar compressive strength was observed as 3.78 MPa. The procedure presented below is illustrated the preparation of the experimental program [10]. PP-bands are arranged in meshes and connected at their intersection points using a portable plastic welder. In this experiment, during construction of the model house, straw is put in the place at the pitch where we required holes. Walls are wrapped by meshes around the corners and wall edges. The overlapping length should be long enough to accommodate sufficient wire connectors as this is the only system used to connect meshes to the structure. Wires are passed through wall holes and used to connect the meshes on both wall sides and a steel piece or any other stiff element is placed between the band and the wire. The bottom edge and top edge of the PP-band mesh should be connected to the structural foundation and roof level, respectively. Fixed connectors around the openings after the mesh were cut and overlapped on the other side.

2.2 Materials used

For the house models, one-quarter scale adobe unit 75 mm × 50 mm × 35 mm in size was used. The adobe materials were manufactured in Japan and used as the raw material for the test models. The adobe was a mixture of Mikawa clay (30%), ceramic waste soil (55%), sand (8%) and ceramic waste (7%). Adobe compressive strength and Young's modulus were observed as 8.05 MPa and 1.68 GPa, respectively. The main target of retrofitting with PP-band mesh is to improve the earthquake-safety of seismically vulnerable masonry houses in developing countries, so it was desirable to use materials with similarly low-strength characteristics in the tests. Because only strong bricks were available due to logistical issues, a very weak mortar mix was used in order to obtain low-strength masonry. Therefore, for the manufacturing of the mortars, mortar designation (iv) mix according to BS EN 1996 [19] was selected. Traditionally, cement-sand mortar and cement-lime-sand mortar were used for masonry joint mortar. Lime has been used in mortar to improve its workability and water retention properties. It was thought that both of these properties were desirable considering possible difficulties in adequately placing mortar in the bed joints with a small thickness in scale models [20]. For joint layers, 5 mm thick cement, lime and sand ratio of 1:2.8:8.5 for the mortar with a cement/water ratio of 33% was used. During construction of the models, specimens were prepared for compression, shear, bond and diagonal shear test to obtain the mechanical properties of the masonry. The layout of specimens used for these tests is shown in Fig. 3.

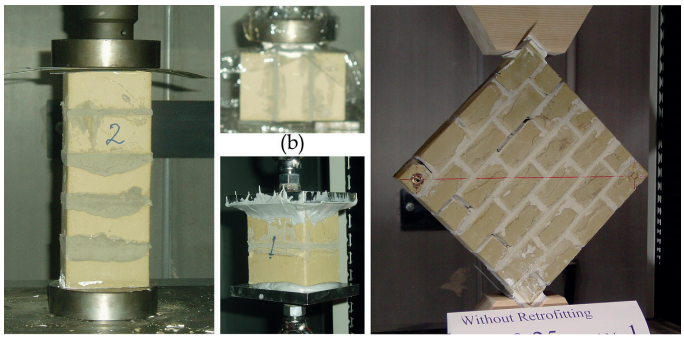

Fig. 3 Testing setup (a) compression test (b) direct shear test, (c) bond test, and (d) diagonal shear test

The axial compression tests, direct shear test, three-point flexural bending tests and diagonal shear tests were performed under displacement control, according to BS EN 1052-1 [21], BS EN 1052-3 [22], BS EN 1052-2 [23] and ASTM E519-10 [24], respectively. The compressive, shear, bond and diagonal shear strength of masonry were listed in Table 1.

Table 1 Specimen mechanical properties

	Specimen		
	1	2	3
Compression strength (MPa)	4.26	4.35	4.36
Shear strength (kPa)	6.4	6.0	6.8
Bond strength (kPa)	4.5	5.1	4.6
Diagonal shear strength (kPa)	42	47	45

PP-bands used in this experimental program shown in Fig 4(a). Tensile testing for the PP-bands was carried out according to ASTM D3822 standard [25] to check its mechanical properties as shown in Fig 4(b)–(d). PP-bands show the average tensile capacity of 172 MPa at 13% axial strain with an initial and residual modulus of elasticity of 3.2 and 1.0 GPa, respectively. Initial and residual modulus of elasticity was calculated by drawing a tangent to the initial and secondary linear portion of the load-extension curve, respectively.

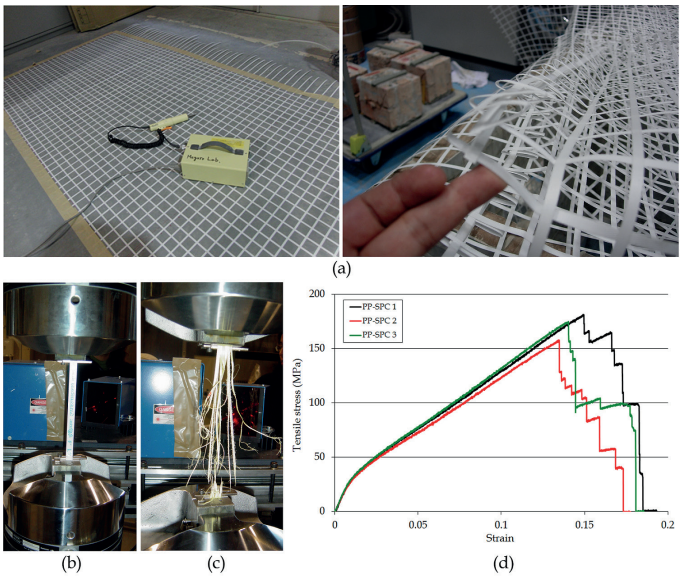

Fig. 4 Retrofitting material (PP-band) (a) preparation of PP-band (b) tensile testing on the PP- band, (c) failure pattern of PP-band and (d) stress-strain behavior of the PP-band under tensile load

2.3 Test procedures and instrumentation

The shaking table system at the University of Tokyo was used for the test. Shaking table has the performances of displacement ± 100 mm, acceleration ± 20 m/s^2, the total payload of 2000 kg and table dimension of 1.5m by 1.5m. The input motion sequence of shaking table test is shown in Table 2. Simple sinusoidal motions with frequencies ranging from 2 Hz to 35 Hz and amplitudes ranging from 0.05 g to 1.4 g were applied to the specimens to obtain the dynamic response of each house model [10]. Figure 5 shows the typical shape of the applied sinusoidal wave input motion. To measure the acceleration and displacement, 24 accelerometers and 5 lasers were installed at the locations shown in Fig. 6.

Table 2 Shaking table rest run sequence

	Frequency (Hz)	35	30	25	20	15	10	5	2
	No of Cycles	80	80	80	80	80	80	50	40
	Sweep				01, 02				
Amplitude	0.05g	03	04	05	06	07	08	09	10
	0.1g	11	12	13	14	15	16	17	18
	0.2g	19	20	21	22	23	24	25	46
	0.4g	26	29	32	35	38	41	44	51
	0.6g	27	30	33	36	39	42	45	52
	0.8g	28	31	34	37	40	43	47	53
	1.0g							48	
	1.2g							49	54
	1.4g							50	

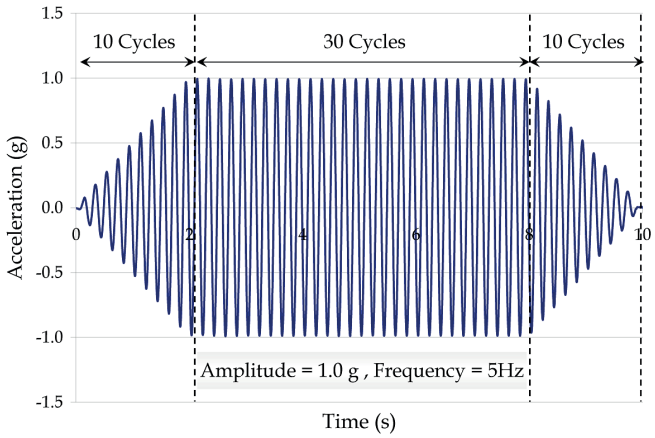

Fig. 5 Input sinusoidal motion

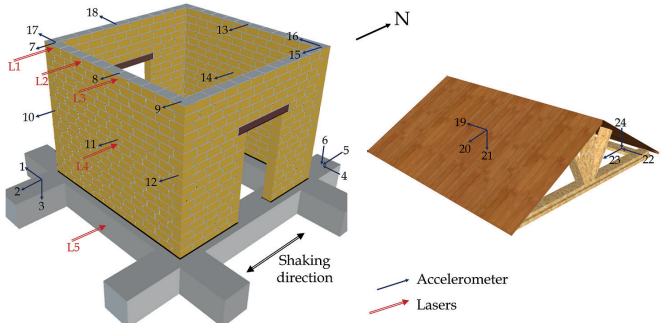

Fig. 6 Accelerometers and lasers position (arrows indicate the positive direction)

3 Performance of the house models

3.1 Model 1

Initial crack and propagation were observed from the corner of the window opening at run 25. Still, there was no major crack observed on walls, which are in the parallel direction of motion. At the end of run 34, many cracks were observed and cracks at the corner of the opening propagate up to the top layer of the wall. Also, there was a major crack observed on walls, which are in the parallel direction of motion as shown in Fig 7(a). At the end of run 37, "X" type crack was observed in both walls, which are in the parallel direction of motion. Also, a lot of cracks observed in the top of the openings.

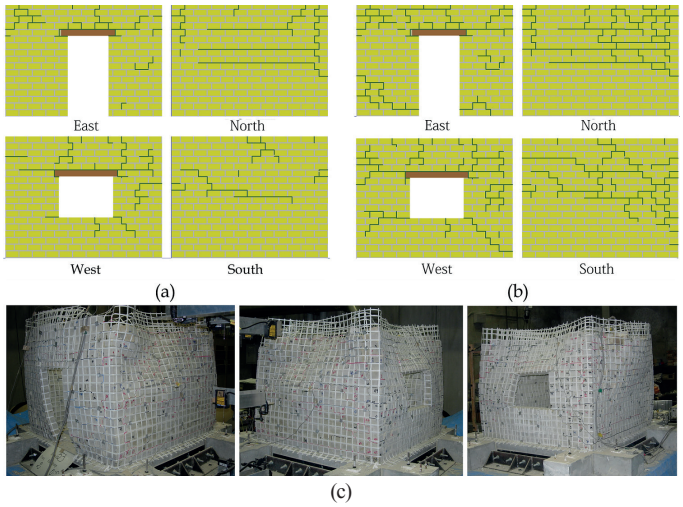

Fig. 7 House model 1 at various levels (a) crack pattern at run 34 (b) crack pattern at run 40 and (c) damage level at the end of run 53

At the end of run 40, a large crack was observed in the walls which are in the orthogonal direction of motion, especially closer to the connection between adjacent wall as shown in Fig 7(b). Although PP-band mesh kept the structure as a single unit during the shaking, it allowed the sliding of the adobe units along these cracks. This behavior was observed even in the following run too. At the end of the run 53, almost all the mortar joints were cracked, the specimen did not lose stability. However, house model showed the excessive permanent deformation on both in-plane and out-of-plane walls as shown in Fig 7(c). Testing stopped at this level due to the shaking table capacity limitation is reached.

3.2 Model 2

For model 2, up to the end of Run 26, no major crack was observed. At the end of the run 27, crack was observed from the top corner of the openings and it propagates up to the top layer of the wall which is in the parallel direction of motion. No cracks are observed in the walls orthogonal to the motion. At the end of run 34, more cracks observed at the top part of the wall with the door opening. Also, one long horizontal crack observed in the top part of the south wall which is in the orthogonal direction of motion as shown in Fig 8(a). At the end of the run 37, vertical crack was observed from the left side of the north wall which is in the orthogonal direction of motion. Also, one long horizontal crack observed in the top part of this wall. At the end of run 40, a vertical crack appears in Run 37 propagates up to the bottom of the wall. The new vertical crack was observed on the right side of the south wall which is in the orthogonal direction of motion. On the west wall, the crack propagates from the bottom corner of the window opening to the bottom corner of the wall which is in the parallel direction of motion as shown in Fig 8(b). At the end of run 43, "X" type crack was observed in both walls, which are in the parallel direction of motion. At the end of run 48, almost all the mortar joints were cracked, but the specimen did not lose stability.

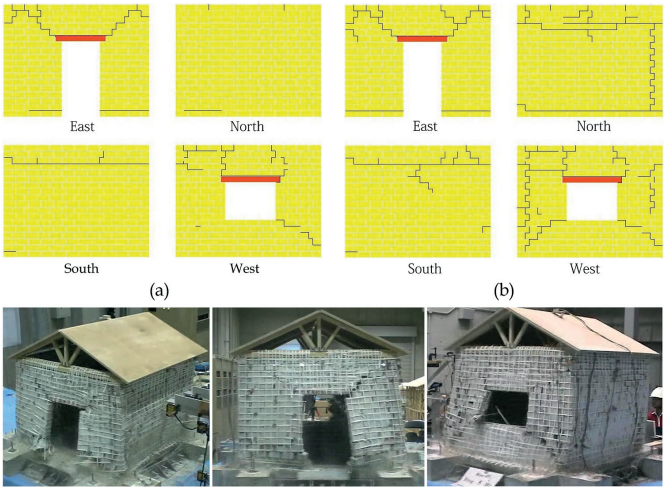

Fig. 8 House model 2 at various levels (a) crack pattern at run 34 (b) crack pattern at run 40 and (c) damage level at run 49

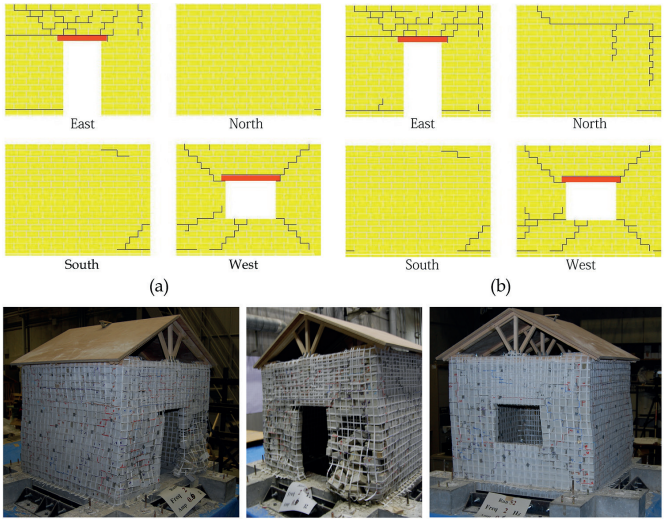

Fig. 9 House model 3 at various levels (a) crack pattern at run 34 (b) crack pattern at run 40 and (c) damage level at the end of run 52

At run 49, due to roof connected to only two walls, house model deformed from the actual shape. Therefore, during shaking, horizontal PP-bands pull inside and due to that in some area (particularly closer to opening) horizontal PP-bands separated from the vertical PP-band. The consequence of that PP-band mesh effect was reduced, and it creates space between inside and outside PP-band mesh. Adobe unit readjusts inside mesh generate permanent gap results in second order effect, which trigger structural instability and its result the total failure of the specimen. This was the last run for Model 2.

3.3 Model 3

Major cracks were observed closer to openings from Run 21, which are in the parallel direction of motion. Figure 9(a) shows the crack patterns for model 3, after run 39.

At first, inclined cracks initiating at the corner of the opening window opening which is in the parallel direction of motion, and it reached the top and bottom layer of the model.

In the east wall which in the parallel direction of motion, where the door is located, the inclined cracks were accompanied by horizontal cracks that reached the wall which is in the orthogonal direction of motion. Each successive shake caused new cracks after run 40 as shown in Fig 9(b). In each loading, the cracks widen and sliding along mortar joints could be clearly observed. In particular, north and south walls, which were subjected to out-of-plane loads, were extensively cracked causing large deformations during shaking. At the final stage of the test, run 52, there is a local failure observed closer to the door opening as shown in Fig 9(c). Testing stopped at this level due to the excessive shaking of the house model.

3.4 Structural performance

The performance of the models was assessed based on the damage level of the buildings described in the European Macroseismic Scale, EMS-98 [26]. EMS-98 categorized the damage level in five as light structural damage, moderate structural damage, heavy structural damage, partial collapse, and collapse. Fig 10 summarized the house models damage level for input shaking motion cooperate with amplitude, frequency and the Japan Meteorological Agency (JMA) seismic intensity scale. The JMA seismic intensity scale was calculated based on the method proposed by Sakai et al. [27].

Until run 47, all three models showed the moderate levels of structural damage. After run 48, house model 2 showed rapid degradation and heavy structural damage during run 48. The total collapse of this model occurred in the next run at intensity JMA 5+. In the case of the other two models (Model 1 and Model 3), damage progressed gradually. These models showed a moderate level of structural damage until 48th run and 50th run for Model 1 and Model 3, respectively. Model 1 and Model 3 showed the heavy structural damage at run 51, resulting in a JMA rating of 6-. Even though partial damage occurred at last test run (run 52, resulting in a JMA rating of 6+), escape routes such as doors and windows were secure for both models. However, the Model 1 shows the excessive permanent deformations compared with Model 3 and it behaved as a cantilever structure with free oscillations. In the case of the Model 3, major damage due to local failure closer to the door opening, rather than overall failure and it is only observed for the last couple of runs.

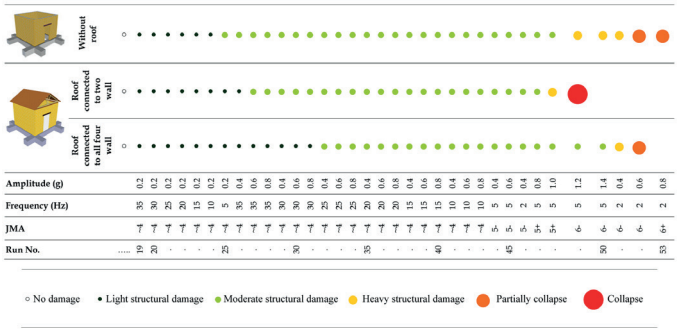

Fig. 10 Performance evaluation based on JMA scale

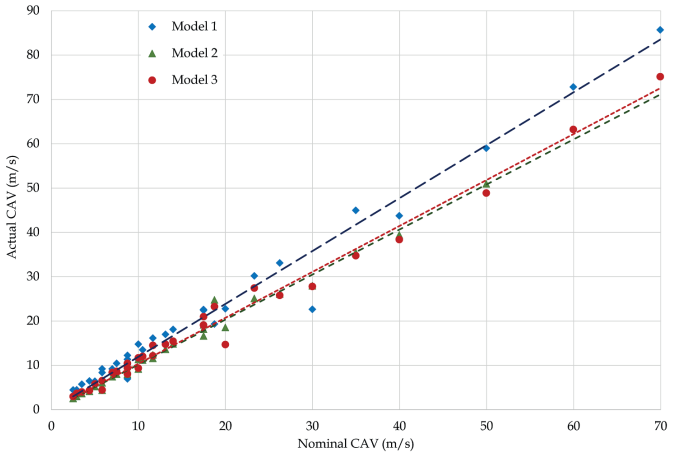

Fig. 11 Plot of actual cumulative absolute velocities vs. nominal cumulative absolute velocities

Based on this result, it can be concluded that a structure with the proper roof connection would be able to control both permanent deformation and local failure compared with house models without box effect or house model with flexible roof connection.

4 Results and discussion

4.1 Vibration response

Cumulative absolute velocity (CAV) is the possible measures of the potential damage to the structures. For each test, the cumulative absolute velocity (CAV) is evaluated as Eq (1).

$$CAV = \int_0^{t_{max}} |a(t)|\,dt \tag{1}$$

where |a(*t*)| is the absolute value of the acceleration time series and t_{max} is the total duration of the shaking table input.

As evident from Fig. 11, the house model 1 was subjected to a much higher cumulative absolute velocity of shaking in comparison to the nominal cumulative absolute velocity, with values that are almost 20% larger than the nominal CAV value. However, house models 2 and 3 shows the actual CAV value closer to reference CAV value.

4.2 Lateral drift

In general, lateral deformation cause to nonstructural elements of the structure. However, for larger lateral deformation, there is the risk of the partial or total collapse of the structures. Lateral story drift is defined by the lateral displacement at the top corner of the wall divided by the height of the wall. Diaphragm drift is defined as mid wall displacement at roof level divided by the length of the wall as shown Fig. 12.

Figures 13 and 14 show the story drift and diaphragm drift correspond to the peak base velocity of shaking table input motion. House models 2 and 3 show the closer behavior in story drift. House model 1 shows the larger lateral drift than the other two models for stronger intensity shaking. Compared with model 1, the lateral story drifts 63% and 66% less for models 2 and 3, respectively. In the case of diaphragm drift, models 2 and 3

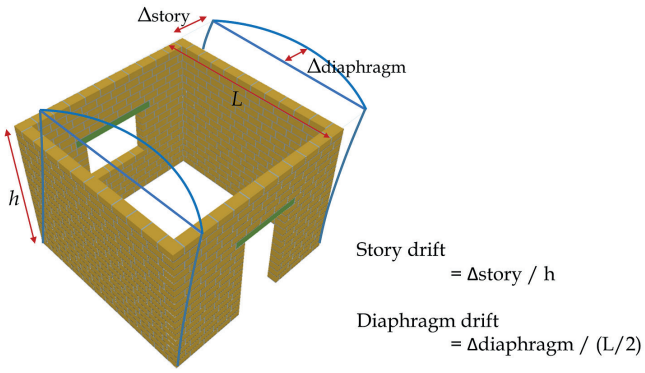

Fig. 12 Define the story drift and diaphragm drift

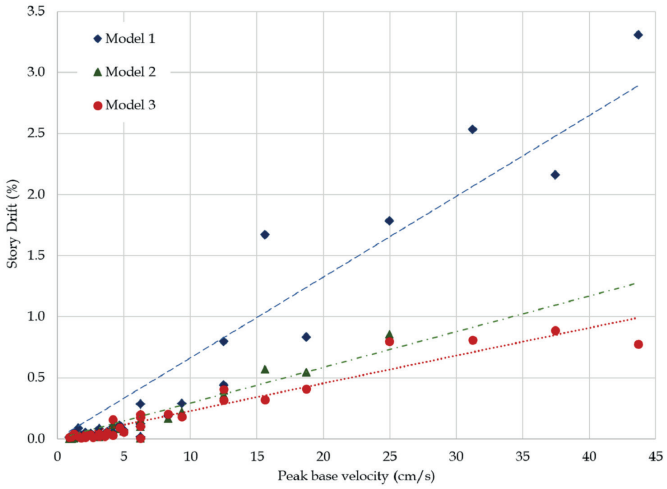

Fig. 13 Story drift variation with the peak base velocity

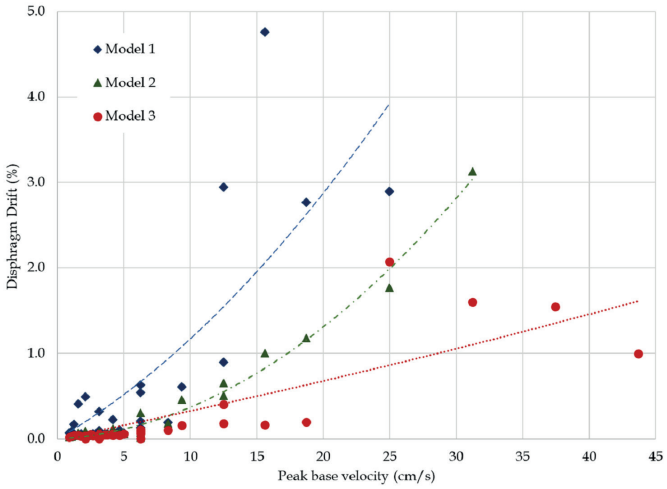

Fig. 14 Diaphragm drifts variation with the peak base velocity

drift 25% and 44% less than that of model 1, respectively. These results show that; better roof diaphragm connection controls both story and the diaphragm deformation of the wall during shaking.

ASCE-41-06 [28] defines the maximum drift levels of 1.5% transient or permanent for a reinforced masonry structure that is under collapse prevention condition. Model 1 exceeds this drift level in-plane direction at 15 cm/s peak base velocity. In the case of out-of-plane, Models 1 and 2 exceed this drift level at 15 cm/s peak base velocity. However, the model 3 shows fewer than 2% lateral drift for even higher intensity motions.

4.3 Shear resistance

The shear resistance of the house model has been analyzed based on the acceleration and displacement response times history data. Lateral shear resistance was computed as the multiple of the measured accelerations and corresponding masses as shown in Eq (2);

$$SS = \sum_{i}^{n} m_i a_i \tag{2}$$

where SS is the lateral shear force, m_i the pertinent mass at each location, a_i the acceleration and n the number of locations selected for calculation.

Figure 15 shows the maximum shear resistance at corresponding lateral drift at roof level for each model. In the elastic range, all three models show the similar shear resistance. Initial shear resistance was 3.09 kN, 2.98 kN and 2.96 kN for house models 1, 2 and 3 respectively. However, post-crack behavior highly influences by a roof and its connection to the house model. Models 1 and 2 show the maximum post-crack shear resistance of 2.63 kN and 2.64 kN, respectively. These resistances are lower than the post-crack shear resistance of model 3, which has 4.16 kN.

4.4 Ductility

The evaluation of the ductility and behavior factor of the house model is based on the approaches suggested by Tomazevic and Weiss [29]. For that, the shear resistance curve has been idealized to the mean of a bilinear approximation based on the equal energy criterion as shown in Fig 16.

The idealized ductility factor and behavior factor are evaluated by Eq (3) and Eq (4), respectively.

$$\mu = d_u / d_e \tag{3}$$

where, d_e is the yield displacement and d_u is the ultimate displacement, at the point where the resistance of the structure decreases to 80% of the maximum.

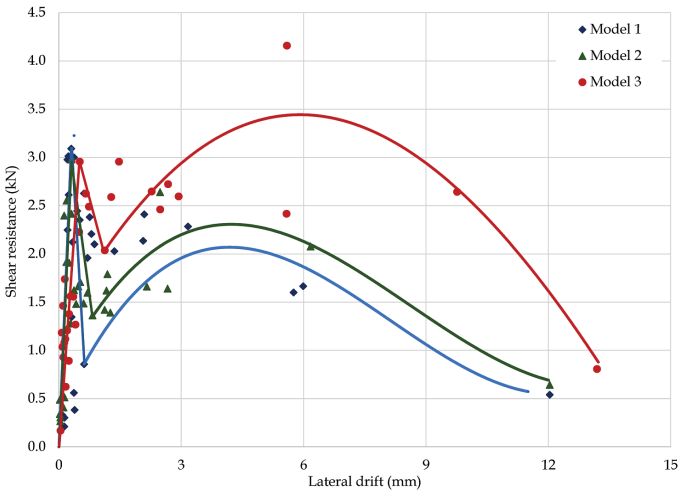

Fig. 15 Shear resistance vs. lateral drift

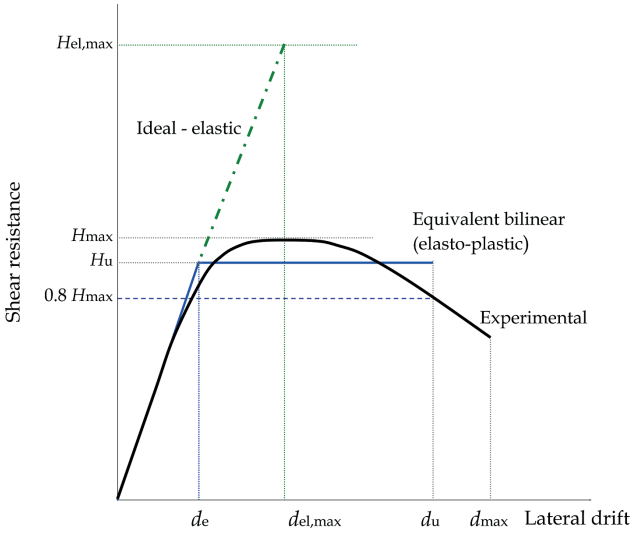

Fig. 16 Shear resistance envelope - bilinear model

Table 3 Seismic response parameters

House model	d_e (mm)	d_u (mm)	$d_{el,max}$ (mm)	H_{max} (kN)	H_u (kN)	$H_{el,max}$ (kN)	μ	q
Model 1	0.31	2.09	0.76	3.09	2.18	7.62	6.74	3.50
Model 2	0.37	4.21	1.70	2.98	2.03	13.73	11.37	6.76
Model 3	0.51	10.34	5.93	2.96	2.89	34.42	20.28	11.90

Table 4 Comparison of important dynamic parameters

	Model 1	Model 2	Model 3
Maximum in-plane drift (%)	3.31	0.86	0.89
Maximum Out-of-plane drift (%)	4.76	3.12	2.08
Pre-crack shear resistance (kN)	3.23	2.98	2.96
Residual shear resistance (kN)	2.63	2.64	4.20

$$q = H_{el,max} / H_u \quad (4)$$

where H_u is the ultimate design load and $H_{el,max}$ is the expected elastic load.

Using the bilinearization method described in Fig. 16, the ductility and behavior factors for each of the models were calculated as shown in Table 3. Results show that both ductility and behavior factors were improved with the box behavior of the house model and the proper roof connection to house models.

5 Conclusions

The effect of roof diaphragm behavior and roof connection on PP-band retrofitted masonry structures were investigated. House models with three different roof conditions: no roof, roof connected to two walls and roof connected to all four walls, were considered for this study. Table 4 summarized the structural performance parameters for each house model.

The obtained results indicate that:

- The roof box behavior and roof diaphragm connectivity played an important role in deciding the failure mode of the masonry structures. PP-band retrofitted house without roof box behavior shows, even though model maintains the integrity, out-of-plane failure is the major issue. However, house model with a roof has shown the local failure than global failure.
- The shear resistance of the masonry house model with the proper roof connection was larger than house model without roof box behavior and house model with improper roof connection.
- Compared with the PP-band retrofitted house made without roof box behavior and improper roof connection; the PP-band retrofitted model with the proper roof diaphragm improve the seismic behavior with respect to lateral drift, shear resistance, stiffness, and ductility.

The test result clearly shows that models with roof diaphragm to wall global response of the structure, preventing the occurrence of local out-of-plane damage mechanisms which occur in the model without a roof. In the present study, even though the roof geometry is scaling down according to the one-quarter scale, low weight roof used in the experimental program is one of the limitations. To simulate the real situation, extra weight has to be attached to the roof of the house model so that the load per unit length of its walls would be similar to that existing in a real house. The negligence of this load is conservative because walls exhibited greater resistance to seismic motions when they were subjected to an additional vertical load.

Acknowledgment

The author acknowledges the Ministry of Education, Culture, Sports, Science and Technology of Japan for extending financial support undertaking the research work. The author wishes to acknowledge Prof. Kimiro Meguro and Dr. Paola Mayorca for providing essential guidelines in the experimental campaign.

References

[1] Coburn, A., Spence R. "Earthquake Protection". (Second Edition), John Wiley & Sons, West Sussex, England, 2002.

[2] Macabuag, J., Guragain, R., Bhattacharya, S. "Seismic retrofitting of non-engineering masonry in rural Nepal". *Proceedings of the Institution of Civil Engineers - Structures and Buildings*, 165(6), pp. 273–286. 2012. https://doi.org/10.1680/stbu.10.00015

[3] Sathiparan, N., Mayorca, P., Meguro, K. "Parametric study on diagonal shear and out of plane behavior of masonry wallettes retrofitted by PP-band mesh". In: *Proceeding of the 14th World Conference on Earthquake Engineering*, Beijing, China. 2008.

[4] Sathiparan, N., Sakurai, K., Numada, M., Meguro, K. "Experimental investigation on the seismic performance of PP-band strengthening stone masonry houses". *Bulletin of Earthquake Engineering*, 11(6), pp. 2177–2196. 2013. https://doi.org/10.1007/s10518-013-9502-z

[5] Sathiparan, N., Sakurai, K., Numada, M., Meguro, K. "Seismic evaluation of earthquake resistance and retrofitting measures for two story masonry houses". *Bulletin of Earthquake Engineering*, 12(4), pp. 1805–1826. 2014. https://doi.org/10.1007/s10518-014-9587-z

[6] Sathiparan, N., Meguro, K. "Strengthening of adobe houses with arch roofs using tie-bars and polypropylene band mesh". *Construction and Building Materials*, 82, pp. 360–375. 2015. https://doi.org/10.1016/j.conbuildmat.2015.02.071

[7] Nesheli, K., Sathiparan, N., Ramesh, G., Mayorca, P., Ito, F., Kagawa, H., Tsugawa, T., Meguro, K. "Full-scale shaking table tests on masonry buildings retrofitted by PP-band meshes". In: *Proceeding of the 5th International Symposium on New Technologies for Urban Safety of Mega Cities in Asia*, Phuket, Thailand. 2006.

[8] Worakanchana, K., Mayorca, P., Guragain, R., Navaratnaraj, S., Meguro, K. "3-D Applied Element Method of PP-band retrofitted masonry". *Seisan Kenkyu*, 60(2), pp. 128–131. 2008. https://doi.org/10.11188/seisankenkyu.60.128

[9] Sathiparan, N. "Mesh type seismic retrofitting for masonry structures: critical issues and possible strategies". *European Journal of Environmental and Civil Engineering*, 19(9), pp. 1136–1154. 2015. https://doi.org/10.1080/19648189.2015.1005160

[10] Sathiparan, N., Mayorca, P., Meguro, K. "Shake table tests on one-quarter scale models of masonry houses retrofitted with PP-band mesh". *Earthquake Spectra*, 28(1), pp. 277–299. 2012. https://doi.org/10.1193/1.3675357

[11] Mayorca, P., Sathiparan, N., Guragain, R., Meguro, K. "Comparison of the seismic performance of different strength masonry structures retrofitted with PP-band meshes". In: *Proceeding of the 5th International Symposium on New Technologies for Urban Safety of Mega Cities in Asia, Phuket*, Thailand. 2006.

[12] Dar, A. M., Umair, S. M., Numada, M., Meguro, K. "Seismic retrofitting of masonry structure with reduced PP-band mesh connectivity". *Seisan Kenkyu*, 55(6), pp. 787–793. 2013. https://doi.org/10.11188/seisankenkyu.65.787

[13] Simsir, C. C., Aschheim, M. A., Abrams, D. P. "Out-of-plane dynamic response of unreinforced masonry bearing walls attached to flexible diaphragms". In: *Proceeding of the 13th World Conference on Earthquake Engineering*, Vancouver B.C., Canada. 2014.

[14] Lourenço, P. B., Mendes, N., Ramos, L. F., Oliveira, D. V. "Analysis of masonry structures without box behavior". *International journal of architectural heritage, Conservation, Analysis, and Restoration*, 5(4–5), pp. 369–382. 2011. https://doi.org/10.1080/15583058.2010.528824

[15] Senaldi, I., Magenes, G., Penna, A., Galasco, A., Rota, M. "The Effect of Stiffened Floor and Roof Diaphragms on the Experimental Seismic Response of a Full Scale Unreinforced Stone Masonry Building". *Journal of Earthquake Engineering*, 18(3), pp. 407–443. 2013. https://doi.org/10.1080/13632469.2013.876946

[16] Magenes, G., Penna, A., Rota, M., Galasco, A., Senaldi, I. E. "Shaking table test of a strengthened full-scale stone masonry building with flexible diaphragms". *International Journal of Architectural Heritage*, 8(3), pp. 349–375. 2014. https://doi.org/10.1080/15583058.2013.826299

[17] Langroudi, J. R., Ranjbar, M. M., Hashemi, S. J., Moghadam, A. S. "Evaluation of roof diaphragm effect on seismic behavior of masonry buildings". In: *Proceeding of the 8th International Conference on Structural Dynamics, EURODYN 2011*, Leuven, Belgium. 2011.

[18] Sathiparan, N. "Effect of roof diaphragm on masonry structures under dynamic loading". *Earthquakes and Structures*, 10(2), pp. 351–366. 2016. https://doi.org/10.12989/eas.2016.10.2.351

[19] BS EN 1996-1-1:2005+A1:2012, Eurocode 6. "Design of masonry structures. General rules for reinforced and unreinforced masonry structures". Brussels: Comité Européen de Normalisation, 2012.

[20] Sathiparan, N., Anjalee, W. A. V., Kandage, K. K. S. "The scale effect on small-scale modeling of cement block masonry". *Materials and Structures*, 49(7), pp. 2935–2946. 2016. https://doi.org/10.1617/s11527-015-0696-1

[21] BS EN 1052-1. "Methods of tests for masonry - Part 1: Determination of compressive strength". British Standards Institution, London, UK. 1999.

[22] BS EN 1052-3. "Methods of test for masonry - part 3: determination of initial shear strength". British Standards Institution, London, UK. 2002.

[23] BS EN 1052-2. "Methods of test for masonry - part 2: determination of flexural strength". British Standards Institution, London, UK. 1999.

[24] ASTM E519. "Standard test method for diagonal tension (shear) in masonry assemblages". Annual Book of ASTM Standards, ASTM International, West Conshohocken PA, USA. 2010.

[25] ASTM D3822 / D3822M-14. "Standard Test Method for Tensile Properties of Single Textile Fibers". Annual Book of ASTM Standards, ASTM International, West Conshohocken PA, USA. 2014.

[26] Grunthal, G. "European Macroseismic Scale (EMS-98)". Centre Europèen de Géodynamiqueet de Séismologie, Luxembourg, UK. 2001.

[27] Sakai, Y., Kanno, T., Koketsu, K. "Proposal of instrumental seismic intensity scale from response spectra in various period ranges". *Journal of Structural and Construction Engineering*, 69(585), pp. 71–76. 2004. https://doi.org/10.3130/aijs.69.71_4

[28] ASCE/SEI Standard 41. "Seismic rehabilitation of existing buildings". American Society of Civil Engineers, Reston, Virginia, USA. 2006.

[29] Tomazevic, M., Weiss, P. "Displacement capacity of masonry buildings as a basis for assessment of behaviour factor: An experimental study". *Bulletin of Earthquake Engineering*, 8(6), pp. 1267–1294. 2010. https://doi.org/10.1007/s10518-010-9181-y